

ROTATION-GAMMA CORRECTION AUGMENTATION ON CNN-DENSE BLOCK FOR AUGMENTATION ON CNN- DENSE BLOCK FOR SOIL IMAGE CLASSIFICATION

by Putri NATASYA

Submission date: 13-Mar-2025 02:20AM (UTC+0700)

Submission ID: 2021090533

File name: OTATION-GAMMA_CORRECTION_AUGMENTATION_ON_CNN-DENSE_BLOCK_FOR.pdf (1.52M)

Word count: 7362

Character count: 38253

Keywords: CNN, Image Classification, Gamma Correction, Rotation, Soil

Sri Indra Maiyanti^{[0009-0009-9983-8279]*}, Anita Desiani^{[000-0001-8851-2454]**},
Syafrina Lamin^{[0009-0007-0499-4013]***}, Puspitashati^{[0009-0000-5548-3992]****},
Muhammad Arhami^{[0000-0002-7992-0103]*****}, Nuni Gofar^{[000-0003-3469-1690]*****},
Destika Cahyana^{[0000-0001-8461-0700]*****}

ROTATION-GAMMA CORRECTION AUGMENTATION ON CNN-DENSE BLOCK FOR SOIL IMAGE CLASSIFICATION

Abstract

Soil is a solid particle that covers the surface of the earth. Soil can be classified based on its color because the color indicates the nature and condition of the soil. CNN works well for image classification, but it requires large amounts of data. Augmentation is a technique to increase the amount of training data with various transformation techniques to the existing data. Rotation and Gamma Correction can be used simply as an augmentation technique and can reproduce an image with as many image variations as desired from the original image. CNN architecture has a convolution layer and Dense block has dense layers. The addition of Dense blocks to CNN aims to overcome underfitting and overfitting problems. This study proposes a combination of Augmentation and classification. In augmentation, a combination of rotation and Gamma correction techniques is used to reproduce image data. The CNN-Dense block is applied for classification. The soil image classification is grouped based on 5 labels black soil, cinder soil, laterite soil, peat soil, and yellow soil. The performances of the proposed method provide excellent results, where accuracy, precision, recall, and F1-Score performances are above 90%. It can be

*Mathematics Departement, Mathematics and Natural Science Faculty, Universitas Sriwijaya, Sri.indra.maiyanti@mipa.unsri.ac.id

**Mathematics Departement, Mathematics and Natural Science Faculty, Universitas Sriwijaya, anita_desiani@unsri.ac.id (corresponding author)

*** Biology Department, Faculty of Mathematics and Natural Science, Universitas Sriwijaya, rinapps@unsri.ac.id

**** Agriculture Technology Departement, Faculty of Agriculture, Universitas Sriwijaya, puspitahati@unsri.ac.id

***** Informatics Technique Departement, Politeknik Negeri Lhokseumawe, Lhokseumawa, Indonesia, Muhammad.arhami@pnl.ac.id

***** Soil Departement, Faculty of Agriculture, Universitas Sriwijaya, nigofar@unsri.ac.id

***** Research Center for Geospasial, Research Organization for Earth Science and Maritime, the National Research and Innovation Agency of the Republic of Indonesia, dest009@brin.go.id

concluded that the combination of rotation and Gamma Correction as augmentation techniques and CNN-Dense blocks is powerful for use in soil image classification.

1. INTRODUCTION

Soil is the top layer of the earth's surface with combinations of solid particles, water, and air. The soil structure consists of mineral, organic, and chemically bound deposits accompanied by liquids and gases that occupy the gaps between the solid particles (Yu et al., 2019). According to (Yu et al., 2019), soils are grouped into various system classifications from one area to another varying according to their characteristics and needs. Soil characteristics have an important role in various tasks in agriculture, one of which is for plant nutrient needs (Taher et al., 2021). However, not all soil is suitable for plant growth. So far, distinguishing soil varieties is done by collecting soil samples and analyzing them manually by experts. However, manual soil determination in all system classification takes a long time, has high accuracy, and is quite expensive (Novakovi et al., 2017). In this case, an automated system is needed to distinguish soil varieties through previously collected soil images.

One of the automated systems with the help of computers in classifying soil varieties is to classify them. Image classification is a process of grouping an object into certain classes based on their similarity of characteristics (Novakovi et al., 2017). The method of soil image classification is done by dividing the number of soil images into different classes based on predetermined characteristics. Taher et al., (2021) used the Naïve Bayes, Decision Tree, and Random Forest methods for soil classification. Unfortunately, the accuracy resulting from this study is still below 70%. Harlianto et al., (2017) applied the Neural Network, Decision Tree, and Naïve Bayes methods for soil classification with accuracy results of 77.65%, 74.12%, and 75.29%. Unfortunately, both studies still used conventional methods and did not measure other performance measures such as Precision, Recall, and F1-Score. The conventional method refers to a non-deep network approach. Conventional methods involve manually engineered features, are easy to use, do not require a lot of data, are suitable for simple data structures such as tabular data, and have relatively fast training times. Unfortunately, the performance of conventional methods is very limited in representing features in complex data structures such as images (Wang & Deng, 2018). One popular method that is widely used, especially in image classification, is deep learning. Deep learning is a method that applies an artificial neural network with more layers to learn patterns automatically so that it can provide decisions or predictions based on the patterns formed (Desiani, Erwin, Suprihatin, Yahdin, et al., 2021). Convolutional Neural Network (CNN) is the most popular deep learning method for image classification (Hang et al., 2019). The CNN method can receive input data that has $m \times n$ dimension (Desiani, Erwin, Suprihatin, Yahdin, et al., 2021). The application of CNN to soil classification has been applied in several studies. Hamzah et al., (2021) applied CNN to soil classification based on color without performing augmentation techniques. This research obtained very good results where accuracy, precision, recall, and F1-Score were above 95%. Unfortunately, this research only classifies soil images into two labels, namely red soil and black soil. Lanjewar & Gurav, (2022) applied CNN-Resnet and CNN-Dense to soil image classification. The results obtained from CNN-Resnet accuracy, precision,

recall, and F1-Score were above 95%, but the performance results from Dense CNN were only 91% on average. This study applies 2 augmentation techniques, namely rotation and flipping, unfortunately, this study only classifies soil images in 4 labels. Kalyani & Prakash,(2022) used CNN to classify hand images with 2 labels without augmentation. The performance results obtained from this research were only 91% for accuracy, precision, recall, and F1-Score. Soil images can not only be classified based on color but also it can be classified based on texture and substances contained in the soil (Hartemink & Minasny, 2014). The amount of training data has an impact on CNN performance (Hamwood et al., 2018). CNN needs a large amount training data. The larger the data, the better the CNN performance in classification (Desiani, Erwin, Suprihatin, Yahdin, et al., 2021). A small amount of data can cause the CNN model to be underfitting or overfitting during training (Erwin et al., 2022).

Unfortunately, the amount of soil image data is still limited and cannot be freely accessed. Data augmentation is a technique of adding data that can help improve model performance and prevent underfitting or overfitting. The data augmentation technique is used to expand the dataset so that the network may be trained as efficiently as possible (Erwin et al., 2022). Augmentation is a method of increasing the number of datasets by altering the original dataset in various ways (Desiani, Erwin, Maiyanti, et al., 2022). Some augmentation techniques are rotation and contrast conversion. Rotation is a geometric technique that rotates the original image clockwise or counter clockwise by applying varying degrees to produce different images. Image contrast enhancement can be used as an augmentation technique because it produces new images that have different lighting and contrast aspects. Image contrast can be changed with Gamma Correction (Thanapol et al., 2020). Gamma correction is a method to change the contrast of an image by classifying the intensity of the image into bright and dark. Gamma correction is not only used to increase or decrease contrast but also to adjust the intensity of the transformation function (Desiani, Erwin, Suprihatin, Adrezo, et al., 2021). Gamma correction can produce images that are different from the original image (Desiani, Erwin, Suprihatin, et al., 2022). The use of Gamma correction as an augmentation technique has been carried out by Rahman et al., (2016) who applied gamma correction to reproduce chest x-ray image data, and Sun et al., (2021) who applied gamma correction to reproduce retinal image data

Another problem with CNN is that it has deep convolution layers. The convolution layer has sparse connections. It means each neuron in the layer is only connected to a small part of the input area(H. Chen et al., 2020). This reduces the number of parameters and allows the model to learn a better representation of the data. However, having too few parameters can lead to underfitting. Another CNN architecture is Dense block architecture. The Dense block consists of dense layers. The dense layer uses linear operations and produces many parameters because each neuron is connected to all neurons (Desiani, Erwin, Suprihatin, et al., 2022). Having too many parameters can also lead to overfitting. Combining the convolution layer in CNN and the dense layer in the Dense Block allows the CNN-Dense block architecture to overcome the shortcomings of each architecture (Huang et al., 2022; Wu et al., 2019). On the Convolutional layer, not all input nodes influence the output node. It makes the convolutional layer more flexible in learning and the weight per layer is expected to be smaller and convergent. However, deeper layers on CNN can cause a vanishing gradient exploded gradient (Abuqaddom et al., 2021). The advantage of Dense blocks is that the model can take all the output in the previous layer as

input for the next layer so the performance of the model drops because the gradient disappears or explodes in deeper layers. The long distance between the input layer and the next layer can cause the information needed to be lost before it reaches the last layer so that the dense layer can store information in the previous layer.

Soil images in this study have 5 varieties, namely Black Soil, Cinder Soil, Laterite Soil, Peat Soil, and Yellow Soil that are provided in Kaggle datasets. The five soil varieties are sample soils in India and have different characteristics in each image, thus requiring a strong classification method that can learn every feature in the image. The proposed method in the study is the combination of augmentation technique and CNN-Dense block architecture. It will be applied to be able to identify every characteristic that exists in the image data of each soil variety and used to meet the needs of training data on the CNN-Dense block architecture. The augmentation method used in this study is rotation and Gamma Correction. In rotation, degrees for augmentation are used randomly between $0^\circ - 35^\circ$. Limitation on the degree of rotation aims to keep objects in the image from changing too much and prevent other features from entering the image. Rotation can be done easily and with randomly selected degrees between $0^\circ - 35^\circ$ allowing the augmentation technique to be carried out as much as possible to produce a more diverse image compared to the flipping technique. The flipping technique can be applied in two ways, namely horizontal flipping and vertical flipping. Gamma correction is widely applied for image enhancement. However, applying gamma correction as an augmentation technique makes it possible to generate more varied images by simply changing the gamma contrast level in the image. Gamma values can vary from 0 to infinity, but most gamma values used range from 0.1 to 5. Variations of different gamma values are capable of performing as many augmentation techniques as possible with different variations. These augmentation techniques are applied to reproduce the data and obtain a more varied image. The CNN-Dense Block is a modification of the CNN architecture where the last layer of CNN (output layer) which uses fully connected layers is replaced with a Dense block layer. The Dense block consists of 2 dense layers. These layers are used to overcome the occurrence of vanishing or exploded gradients. The CNN-Dense block is expected to be able to study multiple patterns in the soil varieties of images if the images are more diverse. The application of augmentation using rotation and Gamma Correction is expected to meet the needs of training data on the CNN-Dense block so that the architecture performance can be optimal. To measure the success of the proposed method, performance parameters such as accuracy, precision, recall, and F1-Score are used. This study also uses G-mean, Cohen's Kappa, Fowlkes-Mallows Index (FMI), and Positive Likelihood Ratio (posLr) to measure the performance of the proposed method in soil image classification. The addition of these performance measures is to ensure that the proposed method provides the best results.

2. MATERIALS AND METHOD

In this study, the method used for soil image classification is the CNN-Dense block architecture. The first step is to collect and describe the data using the soil varieties image dataset. The dataset is then pre-processed data such as changing the size of the data, labeling the data, and splitting the data. After the pre-processing results, the CNN-Dense block architecture was implemented by extracting its features such as the convolutional layer, Pooling Layer, and ReLU activation function, and continued with the classification

process consisting of flatten, dense layer, and Softmax activation function. The next step is the Testing process to test the accuracy of the model in classifying soil varieties so that the results obtained will be contained in the confusion matrix. The results of the evaluation of the model's performance are measured based on the performance of Accuracy, Precision, Recall, and F-1 Score. The workflow of the stages of this research is presented in the form of a flowchart as shown in Fig. 1.

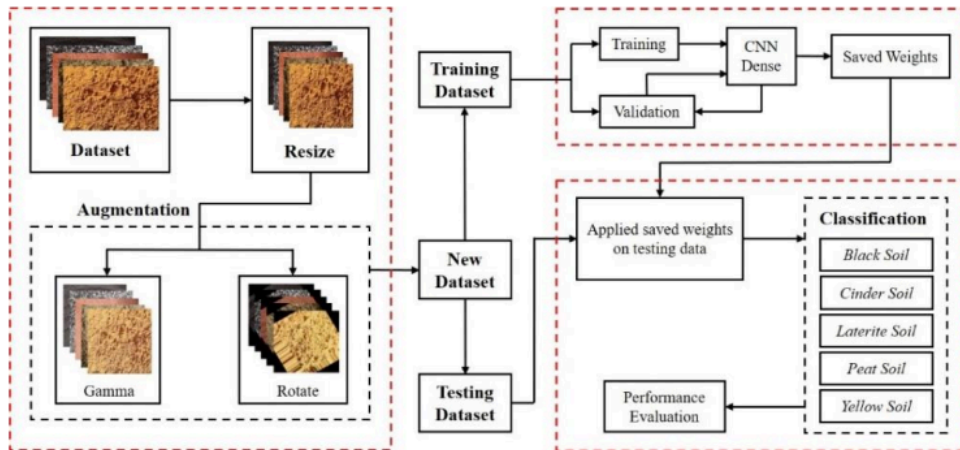


Fig. 1. Workflow of research stages

2.1. Data collection

The data used in this research is the Soil Type Image Classification dataset which is obtained free of charge through the website www.kaggle.com/prasanshasatpathy. The data consists of 156 images of soil varieties which are divided into 5 clusters in 5 folders: 37 images of Black Soil, 30 images of Cinder Soil, 30 images of Laterite Soil, 30 images of Peat Soil, and 29 images of Yellow Soil. Soils were clustered arbitrarily by Prasansa Satpathy who collected soil images in India. The classification of soil data does not refer to soil taxonomy but it uses arbitrary simple classification using color and parent material because this study only tests the opportunity of a Convolutional Neural Network to identify soils and the other concepts of augmentation data can be applied to meet the needs of training data on CNN to classify soil varieties image. Black soil has a specific color: black color; cinder soil is soil that contains large amounts of sand and ash of coal or charcoal; laterite soils are dominated by iron metal content that has a slightly yellowish and reddish red color; peat soil is organic soil that formed in a waterlogged state; and yellow soil is one subsoil that exposed to the surface with specific yellow color. This study uses the Jupyter Notebook software on Anaconda with the Python programming language.

2.2. Data augmentation

2.2.1. Rotation

Rotation is an augmentation technique by applying linear adjustments to image data. In this study, the existing soil images were rotated starting by taking degrees randomly ranging from $0^\circ - 35^\circ$. This is done so that the shape of the soil image is not too different and to avoid the inclusion of new features or colors in the soil image. Fig. 2 is an example of the rotation technique used in this study.

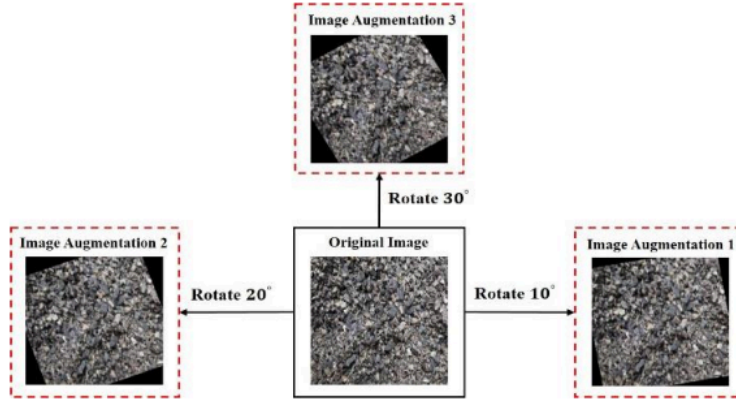


Fig. 2. An example of the application of the rotational augmentation technique on a soil image with different degrees

2.2.2. Gamma correction

Gamma correction determines the output image using Eq. (1) (Desiani, Adrezo, et al., 2022).

$$s_{i,j} = 255 \left(\frac{h_{i,j}}{255} \right)^{\frac{1}{\gamma}} \quad (1)$$

where $s_{i,j}$ is the output result of gamma image correction at (i, j) pixel location, h is the pixel value at (i, j) location of the original image, and γ is the gamma correction value which is determined randomly.

2.3. Training

The amount of data before the augmentation was applied was 156 images. After the augmentation, the number of data increases to 2,500 soil images. Before the training process is carried out using the CNN architecture, the data is first divided by 20%, namely 500 data for testing data and 80% or 2,000 soil images for training data. From the overall training data, the training data was divided by 10% or 200 images as validation data during training.

2.4. Convolutional Neural Network (CNN)

2.4.1. Convolutional Layer

The convolution layer is the main block of CNN which is used to represent feature maps from the input image through a filter consisting of a series of weights. All units in the feature map output have the same filter. For the convolution function shown in Eq. (2) (W. Chen et al., 2020).

$$a_{i,j} = \left(\sum_{u=0}^{n-1} \sum_{v=0}^{n-1} (s_{u+i,v+j} \times k_{i+1,j+1}) \right) + b_q ; i, j = 1, 2, \dots, n \quad (2)$$

where $a_{i,j}$ is feature map on i line and j column, n is the kernel height, $s_{i,j}$ is the input matrix from the gamma correction results, $k_{i,j}$ is the kernel matrix, and b_q is biased for the q -th kernel. The convolution process is carried out with the dot product operation between the submatrix and the kernel using Eq. (2). The multiplication results are then added up and stored into a new matrix called feature maps. This process is repeated until the kernel is at the end of the lower right corner by shifting the kernel by 1 step horizontally and then vertically.

2.4.2. Max pooling layer

The Max Pooling layer is a layer that often follows the convolution layer on CNN, where the image is divided into several parts and takes the maximum value from each part. Max pooling is used to reduce the size of the image dimensions to simplify the next process on CNN.

2.4.3. Rectified linear unit (ReLU)

ReLU is one of the activation functions that can increase training speed in Deep Learning (Desiani, Erwin, Suprihatin, Yahdin, et al., 2021). The ReLU activation function is defined in Eq. (3).

$$r = f(a_{i,j}) = \max(0, a_{i,j}) = \begin{cases} h, & \text{if } a_{i,j} \geq 0 \\ 0, & \text{if } a_{i,j} < 0 \end{cases} \quad (3)$$

where, $a_{i,j}$ is the pixel value of the image from the convolutional operation results and $f(a_{i,j})$ is the output of ReLU activation.

2.4.5. Flatten

Flatten is the process of reshaping a feature map into a vector so that it can be used as input from a dense layer.

2.4.6. SoftMax

Softmax is a combination of several sigmoid activation functions that return a value in the range of 0 to 1, this can be treated as a class-specific data point probability (Sharma et al., 2020). A SoftMax activation function is defined in Eq. (4) (Sharma et al., 2020).

$$s = \sigma(r)_j = \frac{e^{r_j}}{\sum_{j=1}^K e^{r_j}} \quad ; j = 1, 2, \dots, K \quad (4)$$

where r is the output from the ReLU activation function results, $\sigma(r)_j$ is softmax output on input r_j . r_j is the input vector, K is the number of classes in the multi-class classifier.

2.4.7. Loss function (Cross-entropy loss)

Cross entropy loss is a function that is used to calculate the performance of a model by calculating the error generated from the model. The function of Cross-Entropy Loss is shown in Eq. (5).

$$H(p, s) = -\sum_{i=1}^N p_i \log s_i \quad (5)$$

n is the number of rows of the predicted result matrix, s_i is the predicted output matrix entry on label i from the softmax output, p_i is the i^{th} row label entry vector or matrix, and H is the output of the loss function.

2.5. Dense Block

Inside the Dense block, there are dense layers that are interconnected and each layer gets input from the previous layer (Huang et al., 2017). In dense layer consists of convolution operation, batch normalization, ReLU (Rectified Linear Activation), and concatenation operation. At the end of the dense layer, there is a transition layer. The Dense block architecture can be seen in Fig. 3.

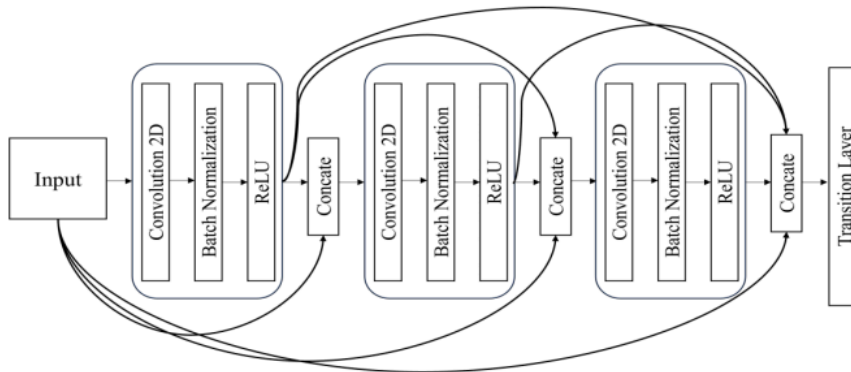


Fig. 3. Dense block architecture

In Fig. 3, the convolution 2D operation is carried out to produce a feature map which will be used as input for the next layer. Batch Normalization is carried out to normalize the feature map results obtained. ReLU is the activation function used in the Dense Layer architecture. The concatenation operation is an operation that merges the output from the previous layer to the next layer. The arrows indicate the direction of the output of each layer which will be concatenated with the output of other layers. The transition layer is a connecting layer between Dense blocks used to control the complexity of the model. The use of Dense blocks is also expected to prevent overfitting. Dense blocks can store all the output of the previous layer as input for the next layer with concatenation operation. The concatenation operation in dense layers can lead to overfitting. To prevent overfitting in dense layers, you can employ feature reuse, dropout, and bottleneck layers. Bottleneck layers typically consists of three main components, namely 1x1 convolution, intermediate layer and dimension expansion.



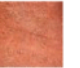


2.6. Testing and evaluation

The testing process is carried out to test the weights generated in the training stage using CNN in classifying soil variety images. The weights generated from the training stage are applied to the testing data and the classification results are measured based on accuracy, precision, recall, F1-Score, G-mean, Cohen's Kappa, Fowlkes-Mallows Index (FMI), and Positive Likelihood Ratio (posLr). The accuracy is used to calculate the accuracy of a model. The precision is used to measure the model's ability to predict positive labels. The recall is used to calculate the positive proportion of both True Positive and False Negative. F1-Score is used to calculate the harmonization of precision and recall. G-mean is used to measure the balance between classification performance on each label. Cohen's Kappa is used to measure the degree of agreement between the resulting predicted label and the actual label on a nominal scale. Fowlkes-Mallows Index (FMI) is used to measure the geometric mean between precision and recall. Positive Likelihood Ratio (posLr) is used to measure the ratio of the probability of getting a positive classification among the set of positive labels and the probability of getting a positive classification among the negative labels.

3. RESULT AND DISCUSSION

In the pre-processing process, the soil image in the soil image dataset is resized to a size of 250×250. Resize is done to equalize the size of the image so that it is easy to process it for the next process. After the resizing process, the image is augmented with data or reproduces the data using a rotation and Gamma Correction. The results of the image augmentation process can be seen in Table 1 for rotation and Table 2 for augmentation with Gamma Correction.

Tab. 1. Rotation augmentation for soil images dataset

No	Degree	Black	Cinder	Laterite	Peat	Yellow
1	Original					

2	20°					
3	30°					

Tab. 2. Gamma correction for data augmentation on soil images dataset

No	Gamma (γ)	Black	Cinder	Laterite	Peat	Yellow
1	Original					
2	0.8					
3	1.2					

In Table 1, it can be seen that there are 5 examples of images that have been carried out by the data augmentation process, where the image is rotated by 20° and 30°. Table 2 shows the application of several different gamma values to the five varieties of soil data. The implementation of rotation and Gamma Correction in the study can generate new data that is different from the original image. The CNN-Dense block architecture in this study can be seen in Fig. 4. Tables 3 and 4 show the histograms resulting from the application of rotation techniques and Gamma values on Gamma Correction. The augmentation process using rotation and Gamma correction can give different images. It can be seen from the histogram generated from the rotation technique and the application of Gamma Correction.

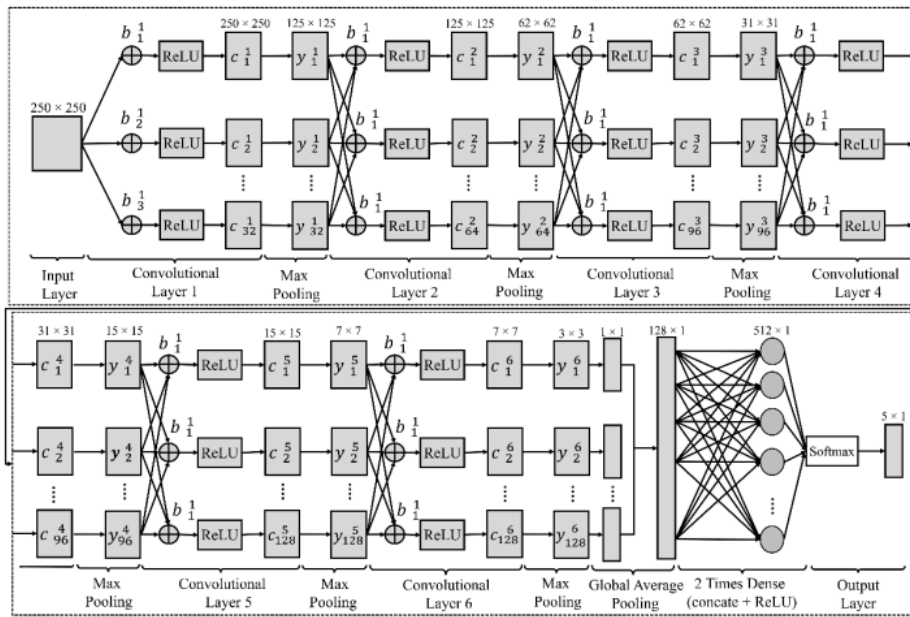

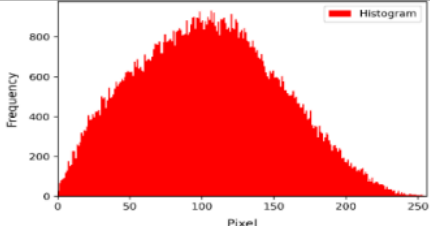

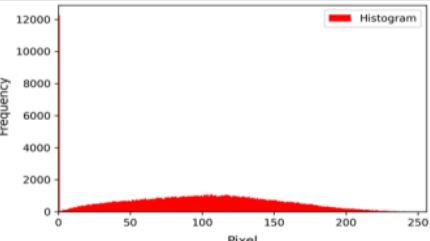


Fig. 4. CNN-Dense block architecture on soil varieties image classification

In Figure 4, it can be seen that the CNN-Dense block architecture consists of an input layer, 6 convolutional layers, 2 Dense blocks, a softmax layer, and an output layer. Each convolutional layer consists of convolution operations, ReLU activation functions, and maxpooling. The result of the 6-th layer convolution has a feature map with a size of 128 x 128. It means that the input to the global average pooling layer is 128x128. An input size of 128x128 means the layer has 128 inputs where each input has 128 feature map channels. The global average pooling calculates the average value of the feature map channel for each input. with a global average pooling, 128 feature map channels are represented by one average value so the output produced on global average pooling is 128x1 in size. The results of the global average pooling operation become input for the 2-Dense block operation. In the Dense block, there are convolution, batch normalization, ReLU activation functions, and concatenation operations to obtain results with dimensions of 512 × 1. The use of neurons in dense layers can be determined freely. This study chooses 512 neurons with the aim of the model being able to describe the input data features in more detail. It allows the model to identify patterns that a simple model might not detect. In this study, a total of 128 inputs from the previous layer are connected through 2 Dense blocks, where each block consists of 512 neurons. During the network training process, the network learns the appropriate weight and bias for each connection of the 128 inputs to 512 neurons through a linear transformation. In the dense layer, a 128x1 input connected to 512 neurons will produce a 512x1 output in the first Dense block. The second Dense block receives input from the first Dense block, namely 512x1, and is connected back to 512 neurons, which will produce the same output, namely 512x1. The final stage is carried out by

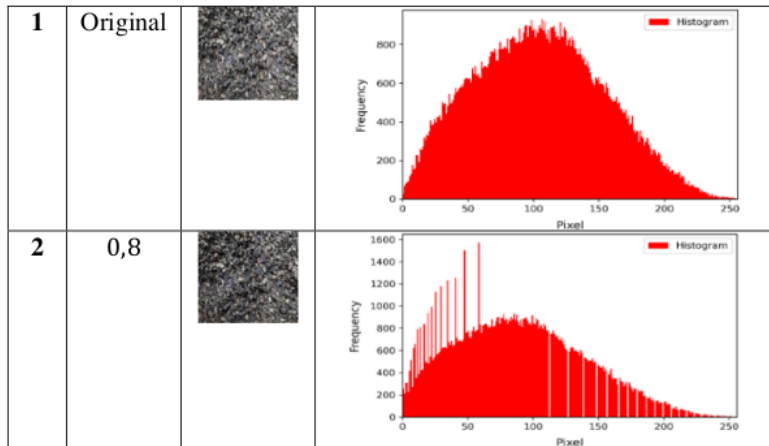
applying the softmax activation function to the Dense block output so that results are obtained with dimensions of 5×1 according to the number of soil data labels in this study. From Tables 3 and 4, it can be ascertained that the augmentation technique used can add new image data to meet the training needs of CNN.

Tab. 3. The comparison of histograms on the original image and the rotated image

No	Degree	Image	Histogram
1	Original		
2	20°		

Tab. 4. The comparison of histograms on the original image and the image resulting from Gamma Correction

No	Degree	Image	Histogram
----	--------	-------	-----------



The sample output on each layer of the CNN-Dense block can be seen in Fig. 5. Fig. 5 shows the output at each layer of the CNN-Dense block architecture. On each layer, the CNN-Dense block tries to get the detailed features that exist in each ground image. The deeper the layer, the smaller the size of the image used because the more detailed the features are taken in the image, every feature of images using the CNN-Dense block architecture, parameters such as the number of epochs is 50 and the batch size is 16. The results of the training data process produce accuracy and loss values in the training data, as well as accuracy and loss values in the validation data. The graph of accuracy and loss obtained in the training data process can be seen in Fig. 6 and Fig. 7.

In Fig. 6(a) it can be seen the graph of the accuracy of the training data and validation data during the training phase. In the first epoch, the accuracy of training data obtained was 0.269 and then increased continuously towards 0.986 at the 50th epoch. The accuracy of validation data in the first epoch obtained a value of 0.747 and continued until the 50th epoch became 0.968. Loss results for training and validation data are shown in Fig. 6(b).

The loss result for training data in the first epoch was obtained at 0.772 and continued to 0.031 at the 50th epoch. The loss result in the first epoch validation data was obtained at 0.689, then decreased to 0.1067 at the 50th epoch. In Fig. 7(a) it can be seen the graph of the recall of the training data and validation data during the training phase. In the first epoch, the recall of training data obtained was 0.6 and then increased continuously towards 0.98 at the 50th epoch. The recall of validation data in the first epoch obtained a value of 0.1 and continued until the 50th epoch became 0.96. Precision results for training and validation data are shown in Fig. 7(b). The precision result for training data in the first epoch was obtained at 0.3 and continued to 0.97 at the 50th epoch. The loss result in the first epoch validation data was obtained at 0.1, then increased to 0.95 at the 50th epoch. The next stage is testing. In the testing stage, the weights of the training process are stored in a model, where the model would be tested for testing data to produce a confusion matrix. Several performances of the model can be calculated by the confusion matrix,

namely accuracy, precision, recall, and F1-Score. Those performances for each label on soil classification are shown in Fig. 10.

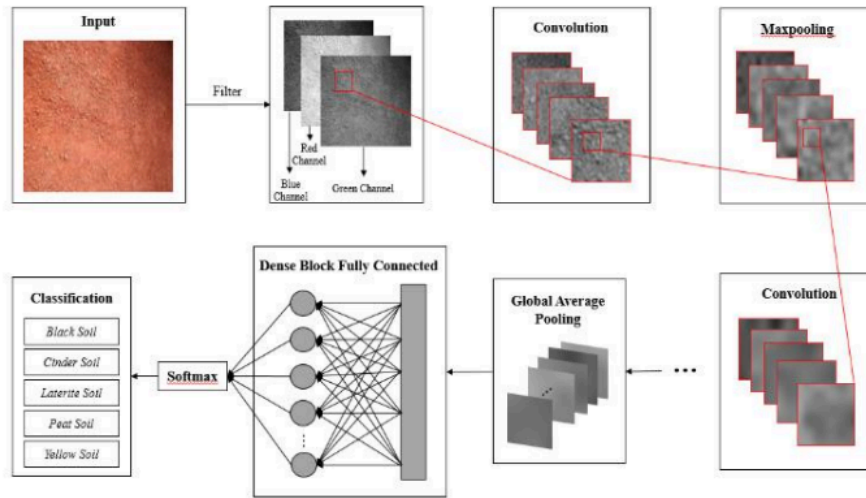


Fig. 5. Output of CNN-Dense block process stages applied to soil varieties image classification

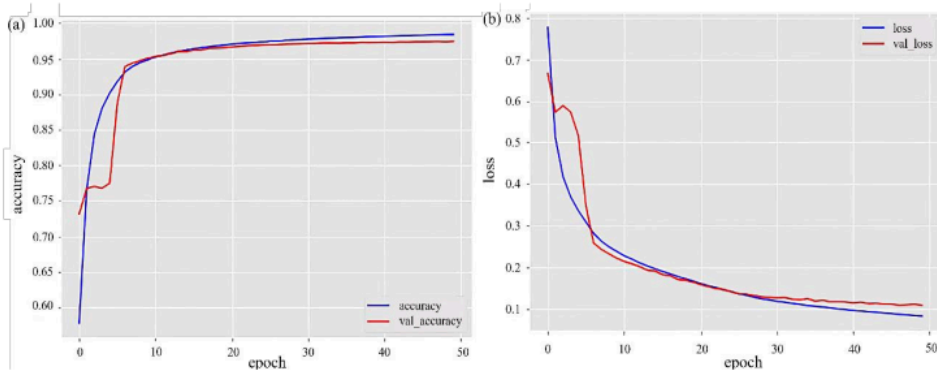


Fig. 6. The graph of (a) accuracy and (b) loss obtained in the training data process

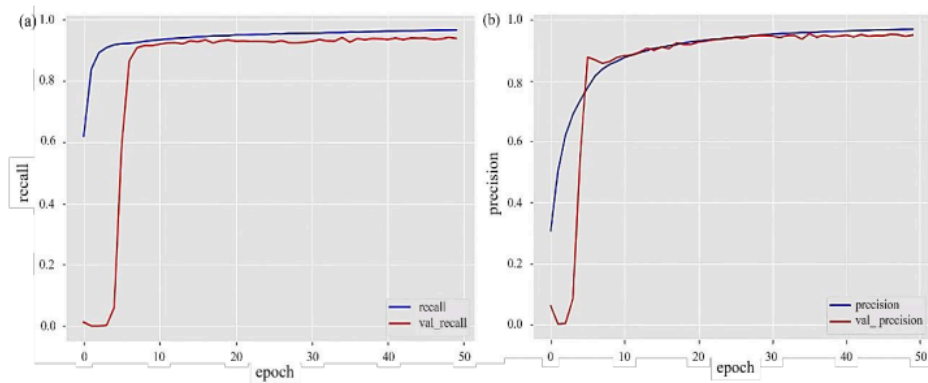


Fig. 7. The results of (a) recall and (b) precision of training data and validation

In Fig. 8, it can be seen that 3 measures of model performance are calculated per soil variety, namely precision, recall, and F1-Score, while the overall accuracy value is calculated. For the black soil, the precision, recall, and F1-Score values are 94%, 91%, and 93%, respectively. For cinder soil, it was 81%, 96%, and 88%, while for peat soil it was 96%, 81%, and 88%. As for laterite soil and yellow soil, the highest value is 100% in the three performance evaluations of the model. In addition, for the overall average value for the five soil varieties, the accuracy, recall, and F1-Score values are 94%, respectively. The success of the CNN-Dense block architectural model in classifying soil varieties can be seen in the ROC graph (Fig. 11). Fig. 9 shows that the CNN-Dense block architecture is excellent at recognizing various soil varieties, namely black, cinder soil, laterite soil, peat soil and yellow soil, where the ROC value of each type is above 0.8. It shows that the application of augmentation using rotation and Gamma correction can improve the performance of the CNN-Dense block architecture.

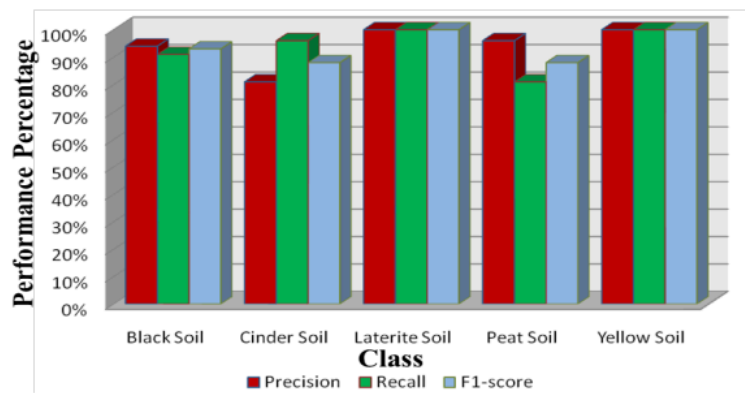


Fig. 8. Results graph of performance evaluation model of CNN-Dense block architecture on soil classification

To measure the success of the CNN-Dense block with rotational augmentation and gamma correction techniques, several other CNN deep learning architectural models were used on the same soil image dataset in this study. The architectural models used are Resnet50 by (He et al., 2016), DenseNet121 by (Huang et al., 2017), Xception by (Chollet, 2017), VGG16 by (Simonyan & Zisserman, 2015) and AlexNet by (Krizhevsky et al., 2012).

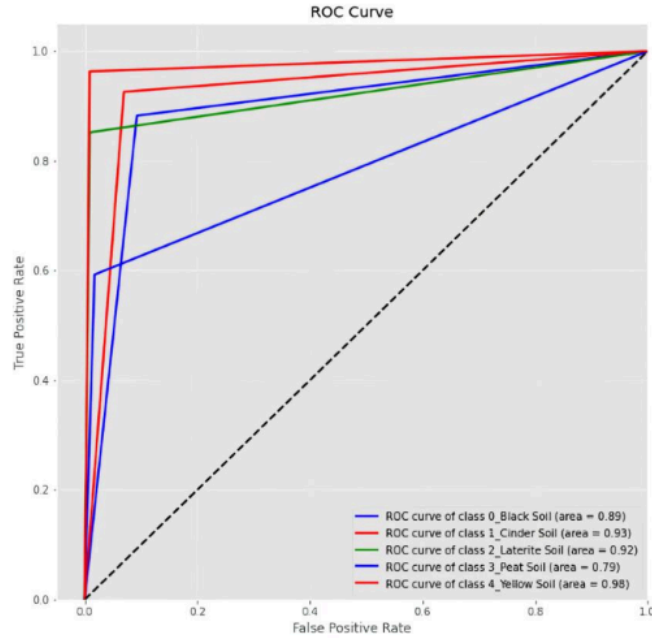


Fig. 9. ROC and AUC for each variety of soil types in the testing data

The performance results of each architecture can be seen in Tables 5 and 6. In Table 5 it can be seen the accuracy (Acc), precision (Pre), recall (Rec), and the F1-Score of each architecture. In Table 6 it can be seen the G-mean, Cohen's Kappa, FMI, and posLr of each architecture. The numbers in bold are the results of the performance evaluation of the architectural model with the highest presentation.

Tab. 5. Comparison of the proposed method with other methods

Method	Result (%)				Total Params
	Acc	Pre	Rec	F1-Score	
ResNet50(He et al., 2016)	79	80	79	79	23.591.685
Dense121(Huang et al., 2017)	89	90	90	90	7.036.357
Xception(Chollet, 2017)	75	74	74	74	20.871.149
VGG(Simonyan & Zisserman, 2015)	70	72	70	70	14.721.989
Alex-Net(Krizhevsky et al., 2012)	69	72	71	69	1.692.613
Our Proposed Method	94	94	94	94	486.277

Tab. 6. Comparison of G-mean, Cohen's kappa, FMI, and posLr on the proposed method with other methods

Method	Result			
	G-mean	Cohen's Kappa	FMI	posLr
ResNet50(He et al., 2016)	0,84	0,93	0,80	0,86
Dense121(Huang et al., 2017)	0,78	0,71	0,71	0,83
Xception(Chollet, 2017)	0,84	0,88	0,74	0,76
VGG(Simonyan & Zisserman, 2015)	0,83	0,98	0,71	0,7
Alex-Net(Krizhevsky et al., 2012)	0,84	0,93	0,90	0,91
Our Proposed Method	0,88	0,76	0,98	0,98

Based on Table 5, the ResNet50 and Xception methods have more than 20 million parameters, but their performance evaluation values are below 80%. Based on Table 6, the highest G-mean, FMI, and posLr are obtained by the proposed method. The highest Cohen's Kappa is obtained by (Simonyan & Zisserman, 2015). Cohen's Kappa on the proposed method is higher than the study by Huang et al., (2017). The method proposed in this study is similar to the AlexNet method but modified with Dense Blocks on the fully connected layer. From Table 5 it can be seen that the highest accuracy, precision, recall, and F1-Score were obtained by the proposed method with less number parameters. The fewer the number of parameters the fewer the complexity of an architecture. These results indicate that the combination of rotational augmentation and gamma correction techniques can meet the training data requirements of the CNN-Dense block to provide excellent performance results. Unfortunately, the rotation technique also has limitations if it is applied carelessly because it can cause loss of information, especially if the rotation is too extensive. Rotation that is too extensive can cause loss of some information such as cropped image angles. It can be a problem if the information in that corner is important for analysis. Gamma correction can not only be used for augmentation but it can also be used to enhance image quality by enhancement image contrast. In gamma correction, over-correction can occur. Correction is the selection of gamma values that are too high or too low. Correction can cause the image to be too bright or too dark. Choosing the wrong gamma value can result in over-correction, which results in an image that doesn't look natural. Based on the study results, it can be seen that the CNN-Dense block architecture can classify data correctly and accurately. This is shown by the accuracy, precision and recall values of 94%. The F1-Score obtained was 94%, this shows a good balance between precision and recall results. The G-mean obtained was 88%, this shows that the classification performance of each label is balanced. The FMI obtained was above 95%, this shows average between precision and recall. Cohen's kappa obtained was 78%, the result is excellent. It means that the agreement is quite good between the predicted labels and the actual labels. The positive probability ratio obtained is 98%, it means that the model is excellent at distinguishing each label. From the performance results obtained, it can be concluded that the proposed method is a robust and excellent method to classify soil images based on their color in five labels, namely black soil, cinder soil, laterite soil, peat soil, and yellow soil.

4. CONCLUSIONS

The augmentation technique in this study uses rotation and Gamma correction. The application of these two techniques can increase the number of soil image data from 156 to 2,500 images. The CNN-Dense block is deep learning that requires a large number of training data. The application of rotation and Gamma correction can improve CNN-Dense block performance in recognizing soil patterns based on images. There are 5 soil varieties that must be identified by CNN-Dense block architecture namely Black Soil, Cinder Soil, Laterite Soil, Peat Soil, and Yellow Soil. The results of performance on each label based on accuracy, precision, recall, and F1-Score all are above 80%. Overall measurements show the average total CNN-Dense block performance on the ground image used is above 94%. This can be concluded with the combination of augmentation techniques and CNN-Dense block architecture is an excellent and robust model to be used in the classification of soil image varieties. The combination of augmentation and CNN-Dense block architecture becomes a model that can be used for the development of intelligent soil image classification applications.

Funding

This research was funded by DIPA of Public Service Agency of Universitas Sriwijaya 2022 SP DIPA 023.17.2.677515/2022, By the Rector's Decree Number 0109/UN9.3.1/SK/2022

Acknowledgments

The authors thank the deep learning discussion group and Computation Laboratory, Mathematics, and Natural Science Faculty Universitas Sriwijaya

Conflicts of Interest

The authors declare that they have no conflict of interest.

REFERENCES

- Abuqaddom, I., Mahafzah, B. A., & Faris, H. (2021). Oriented stochastic loss descent algorithm to train very deep multi-layer neural networks without vanishing gradients. *Knowledge-Based Systems*, 230, 107391. <https://doi.org/https://doi.org/10.1016/j.knosys.2021.107391>
- Chen, H., Chen, A., Xu, L., Xie, H., Qiao, H., Lin, Q., & Cai, K. (2020). A deep learning CNN architecture applied in smart near-infrared analysis of water pollution for agricultural irrigation resources. *Agricultural Water Management*, 240, 106303. <https://doi.org/10.1016/j.agwat.2020.106303>
- Chen, W., Yang, B., Li, J., & Wang, J. (2020). An approach to detecting diabetic retinopathy based on integrated shallow convolutional neural networks. *IEEE Access*, (vol. 8, pp. 178552–178562). IEEE. <https://doi.org/10.1109/ACCESS.2020.3027794>
- Chollet, F. (2017). Xception: Deep learning with depthwise separable convolutions. In *Proceedings of the 2017 IEEE Conference on Computer Vision and Pattern Recognition (CVPR)*, (pp. 1800–1807). IEEE. <https://doi.org/10.1109/CVPR.2017.195>
- Desiani, A., Adrezo, M., Chika Marselina, N., Arhami, M., Salsabila, A., & Gibran Al-Filambany, M. (2022). A combination of image enhancement and U-Net architecture for segmentation in identifying brain tumors on CT-SCAN Images. *2022 International Conference on Informatics, Multimedia, Cyber and Information System (ICIMCIS)*, (pp. 423–428). IEEE.

<https://doi.org/10.1109/ICIMCIS56303.2022.10017519>

- Desiani, A., Erwin, Maiyanti, S. I., Suprihatin, B., Rachmatullah, N., Fauza, A. N., & Ramayanti, I. (2022). R-peak detection of beat segmentation and convolution neural network for arrhythmia classification. *Journal of Engineering Science and Technology (JESTEC)*, 17(2), 1231–1246.
- Desiani, A., Erwin, Suprihatin, B., Adrezo, M., & Alfian, A. M. (2021). A hybrid system for enhancement retinal image reduction. *2021 International Conference on Informatics, Multimedia, Cyber, and Information System, (ICIMCIS)*, (pp. 80–85). IEEE. <https://doi.org/10.1109/ICIMCIS53775.2021.9699259>
- Desiani, A., Erwin, Suprihatin, B., Efriliyanti, F., Arhami, M., & Setyaningsih, E. (2022). VG-DropDNet a robust architecture for blood vessels segmentation on retinal image. *IEEE Access*, (vol. 10, pp. 92067–92083). IEEE. <https://doi.org/10.1109/access.2022.3202890>
- Desiani, A., Erwin, Suprihatin, B., Yahdin, S., Putri, A. I., & Husein, F. R. (2021). Bi-path Architecture of CNN Segmentation and classification method for cervical cancer disorders based on pap-smear images. *IAENG International Journal of Computer Science*, 48(3), 37.
- Erwin, Safmi, A., Desiani, A., Suprihatin, B., & Fathoni. (2022). The augmentation data of retina image for blood vessel segmentation using U-Net convolutional neural network method. *International Journal of Computational Intelligence and Applications*, 21(01), 2250004. <https://doi.org/10.1142/S1469026822500043>
- Hamwood, J., Alonso-Caneiro, D., Read, S. A., Vincent, S. J., & Collins, M. J. (2018). Effect of patch size and network architecture on a convolutional neural network approach for automatic segmentation of OCT retinal layers. *Biomedical Optics Express*, 9(7), 3049–3066. <https://doi.org/10.1364/boe.9.003049>
- Hamzah, Diqi, M., & Ronaldo, A. D. (2021). Effective soil type classification using convolutional neural network. *International Journal of Informatics and Computation*, 3(1), 20–29. <https://doi.org/10.35842/ijicom.v3i1.33>
- Hang, J., Zhang, D., Chen, P., Zhang, J., & Wang, B. (2019). Classification of plant leaf diseases based on improved convolutional neural network. *Sensors*, 19(19), 4161. <https://doi.org/10.3390/s19194161>
- Harlianto, P. A., Adji, T. B., & Setiawan, N. A. (2017). Comparison of machine learning algorithms for soil type classification. *2017 3rd International Conference on Science and Technology - Computer (ICST)*, (pp. 7–10). IEEE. <https://doi.org/10.1109/ICSTC.2017.8011843>
- Hartemink, A. E., & Minasny, B. (2014). Towards digital soil morphometrics. *Geoderma*, 230–231, 305–317. <https://doi.org/10.1016/j.geoderma.2014.03.008>
- He, K., Zhang, X., Ren, S., & Sun, J. (2016). Deep residual learning for image recognition. *2016 IEEE Conference on Computer Vision and Pattern Recognition (CVPR)*, (pp. 770–778). IEEE. <https://doi.org/10.1109/CVPR.2016.90>
- Huang, G., Liu, Z., Maaten, L. Van Der, & Weinberger, K. Q. (2017). Densely connected convolutional networks. *2017 IEEE Conference on Computer Vision and Pattern Recognition (CVPR)*, (pp. 2261–2269). IEEE. <https://doi.org/10.1109/CVPR.2017.243>
- Huang, G., Liu, Z., Pleiss, G., Maaten, L. van der, & Weinberger, K. Q. (2022). Convolutional networks with dense connectivity. *IEEE Transactions on Pattern Analysis and Machine Intelligence*, 44(12), 8704–8716. <https://doi.org/10.1109/TPAMI.2019.2918284>
- Kalyani, N. L., & Prakash, K. B. (2022). Soil color as a measurement for estimation of fertility using deep learning techniques. *International Journal of Advanced Computer Science and Applications*, 13(5), 305–310. <https://doi.org/10.14569/IJACSA.2022.0130536>
- Krizhevsky, A., Sutskever, I., & Hinton, G. E. (2012). Imagenet classification with deep convolutional neural networks. In F. Pereira, C. J. Burges, L. Bottou, & K. Q. Weinberger (Eds.), *Advances in Neural Information Processing Systems 25*. Curran Associates.
- Lanjewar, M. G., & Gurav, O. L. (2022). Convolutional neural networks based classifications of soil images. *Multimedia Tools and Applications*, 81, 10313–10336. <https://doi.org/10.1007/s11042-022-12200-y>
- Novakovi, J. D., Veljovi'c, A., Ili', S. S., Papic, Z., & Milica, T. (2017). Evaluation of classification models in machine learning. *Theory and Applications of Mathematics & Computer Science*, 7, 39–46.

- Rahman, S., Rahman, M. M., Abdullah-Al-Wadud, M., Al-Quaderi, G. D., & Shoyaib, M. (2016). An adaptive gamma correction for image enhancement. *Eurasip Journal on Image and Video Processing*, 35, 2016. <https://doi.org/10.1186/s13640-016-0138-1>
- Sharma, S., Sharma, S., & Athaiya, A. (2020). Activation functions in neural networks. *International Journal of Engineering Applied Sciences and Technology*, 4(12), 310–316. <https://doi.org/10.33564/ijeast.2020.v04i12.054>
- Simonyan, K., & Zisserman, A. (2015). *Very deep convolutional networks for large-scale image recognition*. arXiv. <https://doi.org/10.48550/arXiv.1409.1556>
- Sun, X., Fang, H., Yang, Y., Zhu, D., Wang, L., Liu, J., & Xu, Y. (2021). Robust retinal vessel segmentation from a data augmentation perspective. In H. Fu, M. K. Garvin, T. MacGillivray, Y. Xu, & Y. Zheng (Eds.), *Ophthalmic Medical Image Analysis* (vol. 12970, pp. 189–198). Springer. https://doi.org/10.1007/978-3-030-87000-3_20
- Taher, K. I., Abdulazeez, A. M., & Zebari, D. A. (2021). Data mining classification algorithms for analyzing soil data. *Asian Journal of Research in Computer Science*, 8(2), 17–28. <https://doi.org/10.9734/ajrcos/2021/v8i230196>
- Thanapol, P., Lavangnananda, K., Bouvry, P., Pinel, F., & Leprévost, F. (2020). Reducing overfitting and improving generalization in training convolutional neural network (CNN) under limited sample sizes in image recognition. *2020 - 5th International Conference on Information Technology (InCIT)*, (pp. 300–305) IEEE. <https://doi.org/10.1109/InCIT50588.2020.9310787>
- Wang, M., & Deng, W. (2018). Deep visual domain adaptation: a survey. *Neurocomputing*, 312, 135–153. <https://doi.org/10.1016/j.neucom.2018.05.083>
- Wu, C., Zou, Y., & Zhan, J. (2019). DA-U-Net: Densely connected convolutional networks and decoder with attention gate for retinal vessel segmentation. *IOP Conference Series: Materials Science and Engineering*, 533, 012053. <https://doi.org/10.1088/1757-899X/533/1/012053>
- Yu, H., Zou, W., Chen, J., Chen, H., Yu, Z., Huang, J., Tang, H., Wei, X., & Gao, B. (2019). Biochar amendment improves crop production in problem soils: A review. *Journal of Environmental Management*, 232, 8–21. <https://doi.org/10.1016/j.jenvman.2018.10.117>

ROTATION-GAMMA CORRECTION AUGMENTATION ON CNN-DENSE BLOCK FOR AUGMENTATION ON CNN-DENSE BLOCK FOR SOIL IMAGE CLASSIFICATION

ORIGINALITY REPORT

5%

SIMILARITY INDEX

4%

INTERNET SOURCES

2%

PUBLICATIONS

0%

STUDENT PAPERS

MATCH ALL SOURCES (ONLY SELECTED SOURCE PRINTED)

1%

★ www.etd.dbu.edu.et

Internet Source

Exclude quotes Off

Exclude matches < 1%

Exclude bibliography On

ROTATION-GAMMA CORRECTION AUGMENTATION ON CNN-DENSE BLOCK FOR AUGMENTATION ON CNN-DENSE BLOCK FOR SOIL IMAGE CLASSIFICATION

GRADEMARK REPORT

FINAL GRADE

GENERAL COMMENTS

/0

PAGE 1

PAGE 2

PAGE 3

PAGE 4

PAGE 5

PAGE 6

PAGE 7

PAGE 8

PAGE 9

PAGE 10

PAGE 11

PAGE 12

PAGE 13

PAGE 14

PAGE 15

PAGE 16

PAGE 17

PAGE 18

PAGE 19

PAGE 20
